Published in final edited form as:
Mol Pharm. 2012 July 2; 9(7): 2103–2110. doi:10.1021/mp2005388.

Folic acid-Functionalized Nanoparticles for Enhanced Oral Drug Delivery

Emilie Roger[1], **Stephen Kalscheuer**[1], **Ameya Kirtane**[1], **Bharath Raja Guru**[1], **Alex E. Grill**[1], **Judith Whittum-Hudson**[2], and **Jayanth Panyam**[1,3,*]

[1]Department of Pharmaceutics, University of Minnesota, Minneapolis, MN 55455

[2]Department of Immunology and Microbiology, School of Medicine, Wayne State University, Detroit, MI 48201

[3]Masonic Cancer Center, Minneapolis, MN 55455

Abstract

The oral absorption of drugs that have poor bioavailability can be enhanced by encapsulation in polymeric nanoparticles. Transcellular transport of nanoparticle-encapsulated drug, possibly through transcytosis, is likely the major mechanism through which nanoparticles improve drug absorption. We hypothesized that the cellular uptake and transport of nanoparticles can be further increased by targeting the folate receptors expressed on the intestinal epithelial cells. The objective of this research was to study the effect of folic acid functionalization on transcellular transport of nanoparticle-encapsulated paclitaxel, a chemotherapeutic with poor oral bioavailability. Surface-functionalized poly(D,L-lactide-co-glycolide) (PLGA) nanoparticles loaded with paclitaxel were prepared by the interfacial activity assisted surface functionalization technique. Transport of paclitaxel-loaded nanoparticles was investigated using Caco-2 cell monolayers as an *in vitro* model. Caco-2 cells were found to express folate receptor and the drug efflux protein, p-glycoprotein, to high levels. Encapsulation of paclitaxel in PLGA nanoparticles resulted in a 5-fold increase in apparent permeability (P_{app}) across Caco-2 cells. Functionalization of nanoparticles with folic acid further increased the transport (8-fold higher transport compared to free paclitaxel). Confocal microscopic studies showed that folic acid-functionalized nanoparticles were internalized by the cells and that nanoparticles did not have any gross effects on tight junction integrity. In conclusion, our studies indicate that folic acid functionalized nanoparticles have the potential to enhance the oral absorption of drugs with poor oral bioavailability.

Keywords

Targeted delivery; Oral bioavailability; polymeric systems; folic acid; Caco-2 cells

1. Introduction

Oral administration is the most convenient route of drug delivery. However, poor solubility, low intrinsic permeability across cell membranes, efflux transport, and extensive gut/hepatic metabolism limit the oral bioavailability of many drugs [1, 2]. There has been a longstanding interest in the use of polymeric nanoparticles as drug carriers for overcoming these obstacles [3]. Several groups have showed improved oral bioavailability of encapsulated drugs using nanoparticles formulated with poly(D,L-lactide-co-glycolide) (PLGA) polymer [4–11]. It

*Author for correspondence: Department of Pharmaceutics, College of Pharmacy, University of Minnesota, 308 Harvard Street SE, Minneapolis, MN 55455, Phone: 612-624-0951, Fax: 612-626-2125, jpanyam@umn.edu.

is generally assumed that this increased oral bioavailability is because of uptake into and possible transcytosis of nanoparticle-encapsulated drug across enterocytes and microfold cells [12–14]. Further, because the drug is encapsulated in the nanoparticle matrix, it is protected from enzymatic degradation and drug efflux [15].

Active nanoparticle uptake by enterocytes could be mediated through one or more of the endocytic processes: macropinocytosis, clathrin-mediated endocytosis, caveolae-mediated endocytosis and/or clathrin- and caveolae-independent endocytosis [16]. However, caveolae-mediated endocytosis appears to be the most important mechanism for transcellular transport of nanoparticles [17]. Several proteins are known to initiate caveolae-mediated endocytosis: folic acid receptor, glycophosphatidylinositol anchor, autocrine motility factor receptor, interleukin-2 receptor, GM1 gangliosides, $\alpha_2\beta_1$-integrin, platelet-derived growth factor receptor, epidermal growth factor receptor, and the CCK receptor [13, 15]. Incorporation of ligands onto nanoparticles that could bind to these cell surface proteins could enable transcytosis of nanoparticles and enhance the oral absorption of encapsulated drug [13].

The purpose of the present work was to investigate the potential of folic acid receptor-targeted nanoparticles to improve the oral bioavailability of paclitaxel, a drug with poor oral bioavailability [1, 2]. Folic acid functionalized PLGA-nanoparticles, loaded with paclitaxel, were prepared by the Interfacial Activity Assisted Surface Functionalization (IAASF) technique previously described by our lab [18]. Caco-2 cell monolayers were used as a model intestinal barrier to determine the effect of folic acid functionalization on nanoparticle transport across the intestinal epithelial cells.

2. Materials and methods

2.1 Materials

PLGA (lactide-to-glycolide ratio of 50:50 and average molecular weight of 38 kDa) was purchased from Absorbable Polymers (Pelham, AL). Folic acid, biotin, polyvinyl alcohol (PVA; average MW 30,000–70,000 Da), 6-coumarin, paclitaxel, dimethyl sulfoxide (DMSO), triethylamine, dicyclohexylcarbodimide, N-hydroxy-succinimide, stannous-2-ethyl-hexonate, dicyclohexylurea, phosphotungstic acid, and monoclonal anti-folic acid antibody were obtained from Sigma (St. Louis, MO). α-amine-υ-hydroxy PEG was obtained from Laysan Bio, Inc. (Arab, AL). HPLC grade organic solvents were from Fisher Scientific (Pittsburgh, PA). Cell culture reagents were obtained from Sigma and Invitrogen Corporation (Carlsbad, CA).

2.2 Methods

2.2.1 Preparation of nanoparticles—PLA-PEG (with methoxy terminated PEG) copolymer and PLA–PEG–folic acid were synthesized using previously reported synthetic schemes and characterized by ^{1}H-NMR [19, 20]. PLGA nanoparticles surface-functionalized with PLA-PEG or PLA-PEG-folic acid were prepared by the IAASF technique we previously reported [19]. PLGA (30 mg) was dissolved in 1 mL of chloroform. An oil-in-water emulsion was formed by sonication of the chloroform/polymer solution with 6 mL of 2.5% w/v aqueous PVA solution using a probe sonicator (Sonicator™ XL, Misonix, NY) for 5 min over an ice bath. PLA-PEG copolymer or PLA–PEG-folic acid conjugate were dissolved in chloroform (8 mg in 100 μL) and added to the above emulsion with stirring. The emulsion was then stirred for 18 h at ambient conditions, followed by for 2 h under vacuum to remove chloroform. Nanoparticles were recovered by ultracentrifugation (148,000x*g* for 35 min at 4° C, Optima™ LE-80 K, Beckman, Palo Alta, CA) and washed three times with deionized water. Nanoparticle suspension was then lyophilized (−80° C and <10 mm mercury pressure, Labconco, FreeZone 4.5, Kansas City, MO). To prepare paclitaxel- and 6-

coumarin-loaded nanoparticles, paclitaxel (1 mg) or 6-coumarin (400 μg) was dissolved along with PLGA in chloroform and processed as described above.

2.2.2 Characterizations of nanoparticles—The size distribution and zeta potential of nanoparticles was determined in deionized water (pH ~6.5) using Brookhaven 90 Plus instrument. For scanning electron microscopy (SEM), a sample of nanoparticles was suspended in water (0.5 mg/mL) and placed on to a copper grid. After drying, particles were visualized by using a JEOL 6700 scanning electron microscope. Paclitaxel loading in nanoparticles was determined by methanol extraction of nanoparticles and HPLC analysis of the methanol extract for paclitaxel concentration as described previously [21]. The presence of PLA-PEG co-polymer or PLA-PEG-folic acid conjugate in nanoparticles was confirmed by ^{1}H-NMR. Free folic acid, PLA-PEG-folic acid or nanoparticles were dissolved in NMR grade DMSO-d6 and analyzed using a Varian 400 MHz NMR instrument.

2.2.3 Analysis of folate receptor expression in Caco-2 cells by flow cytometry —The human colon adenocarcinoma cell line (Caco-2) was obtained from the American Type Culture Collection (Manassas, USA) and used between passages 5 and 8. Cells were cultured in Dulbecco's modified Eagle medium (DMEM, high glucose) supplemented with 15% v/v fetal bovine serum, 1% v/v non-essential amino acids, 1% v/v sodium pyruvate, and 1% antibiotic solution in a humidified 5% CO_2/95% air atmosphere at 37° C. Cells were plated on 75 cm^2 flask at a density of 1×10^6 cells/flask and harvested at 80% confluence for all the studies below. To determine folate receptor expression, Caco-2 monolayers were washed in PBS and trypsinized (Tryp LE express, Life Technologies). About 250,000 cells were transferred into tubes for antibody staining. Cells were incubated on ice for 30 min with 100 μL of FACS buffer (1% BSA and 0.1% sodium azide in PBS) containing 2 μg of either purified mouse IgG2b k isotype (BD Pharmingen, 555740) or mouse mAb to folate receptor (Abcam, ab3361). Cells were washed, pelleted, and resuspended in 100 μL of FACS buffer containing 2 μg of FITC labeled goat – anti-mouse secondary antibody (BD Pharmingen, 554001), and further incubated for 30 min on ice. Flow cytometric analysis was carried out on a BD FACScalibur flow cytometer with 488 Laser 530/30 (FL-1) to enable FITC discrimination. Flow data was analyzed on Cyflogic software.

2.2.4 Determination of P-glycoprotein (P-gp) expression by Western blotting—Cells were lysed using 1X RIPA buffer (Thermo Scientific). Protein content was determined using BCA protein assay kit (Thermo Scientific). Proteins (13 μg) were separated by SDS-PAGE on a 4–15% gradient gel and then transferred onto a nitrocellulose membrane using the BioRad Criterion system. The blot was incubated overnight with anti-P-gp antibody (1:50 dilution, Alexis), and then with anti-mouse IgG-HRP linked secondary antibody (1:5000, Calbiochem). HRP linked anti- β-actin antibody (1:5000 dilution, Sigma) was used to probe for β-actin, which served as the loading control. Bands were visualized with SuperSignal West Pico Chemiluminescent Substrate (Thermo Scientific). Band optical densities were determined using ImageJ and Origin software.

2.2.5 In vitro transport of nanoparticles across Caco-2 cell monolayer—For transport studies, cells were seeded on polycarbonate membrane filters (0.4 μm pore size, 1.12 cm^2 growth area) inside Transwell® cell culture chambers (Corning Costar, Cambridge, MA) at a density of 1×10^5 cells/insert. Culture medium (0.5 mL per insert and 1.5 mL per well) was replaced every other day for the first two weeks and everyday thereafter. After 21 – 23 days in culture, cell monolayers were used for the transport study. Before experiments, cell monolayers were washed twice with Hank's buffered salt solution (HBSS) for 15 min at 37° C. The transepithelial electrical resistance (TEER) of monolayers was measured before

and after each experiment by using a Millicell®-ERS-2 system (Millipore Corporation, Bedford, MA). Only cell monolayers with TEER values over 250 Ω cm^2 were used.

The transport of different nanoparticle formulations and free paclitaxel were studied from the apical to basolateral direction in Caco-2 cells. Test solutions consisted of 0.25 mg/mL of nanoparticles (corresponding to 5 μM paclitaxel concentration) diluted in HBSS. Each experiment was started by adding 0.5 mL of test solution to the apical side and 1.5 mL of HBSS to the basolateral side of the Transwell inserts. The cells were then incubated at 37° C and samples were taken at various time points from the basolateral side during the incubation and from the apical side at the end of the study for LC-MS/MS analysis of paclitaxel [19]. Docetaxel was used as the internal standard. A capillary HPLC system (Agilent, CA) coupled to a TSQ Quantum discovery Max triple-quadrupole mass spectrometric detector (Thermo Scientific), equipped with an electrospray ionization source was used. Samples were separated using an Agilent C18 XDB column (50 mm × 4.6 mm, 1.8 μm particle size) that was maintained at 35° C. Analytes were eluted at a flow rate of 0.5 mL/min, using a gradient mobile phase composed of 10 mM ammonium acetate (pH 4.0) and acetonitrile run at initial ratio of 45:55 (buffer: organic solvent) and reaching 100% acetonitrile at 4 min. The total run time was 9 min. Retention time of paclitaxel was at 2.8 min and docetaxel at 3.5 min. The mass spectrometer was run in electrospray positive mode and source conditions were as follows: capillary voltage, 35 V; spray voltage, 3.5 kV; capillary temperature, 250° C; sheath gas pressure, 22 psi; source collision energy, 43 V and collision gas pressure, 1.0 mTorr. SRM mode detected the following transitions: m/z 854.5→286.2 for paclitaxel and m/z 830.3→549.1 for docetaxel. The chromatographic data were acquired and analyzed using Xcaliber software (Thermo Finnigan).

The apparent permeability coefficient (P_{app}), expressed in centimeters per second, was calculated according to the following equation [22, 23]:

$$P = \frac{dQ}{dt}\left(\frac{1}{AC_0}\right)$$

where dQ/dt is the rate of drug appearance on the basolateral side (μg s^{-1}), C_0 is the initial concentration on the apical side (μg mL^{-1}) and A is the surface area of monolayer (cm^2).

To determine paclitaxel accumulation in the cells, the bottom of the filter insert was dried using an absorbent filter paper to eliminate any basolateral medium, and the cell monolayers were washed twice with ice-cold phosphate buffered saline (PBS, 10 mM phosphate buffer, 2.7 mM KCl; 137 mM NaCl; pH 7.5). Cells were then lysed using 0.3 mL of lysis buffer (1% Triton X-100, 5 mM EDTA in PBS). Cell lysates were lyophilized and paclitaxel in the lyophilized samples was extracted with a 45:55 solvent mixture composed of 10 mM ammonium acetate (pH 4.0) and acetonitrile. The extract was then subjected to LC-MS/MS analysis as described earlier. Percent paclitaxel accumulation was calculated as the percent of initial quantity of paclitaxel added on the apical side that accumulated inside the cells.

2.2.6 Nanoparticle uptake in Caco-2 cells—Nanoparticles labeled with 6-coumarin were used to follow their intracellular uptake and trafficking in Caco-2 cells. Extensive studies by several groups have shown the usefulness of 6-coumarin as a fluorescent probe for polymeric nanoparticles for qualitative (microscopy) and quantitative studies *in vitro* and *in vivo* [24–27]. 6-coumarin is a highly lipophilic molecule and does not leach out of nanoparticles in the time frame of the study. Previous studies have shown that less than 0.1% of the encapsulated molecule is released in 48 hrs [28]. After incubation with 0.25 mg/mL nanoparticles dispersed in HBSS at 37° C for 2 h and 6 h, cell monolayers were washed

three times with HBSS. Cell monolayers were then fixed with 4% paraformaldehyde solution, rinsed with PBS, and permeabilized using 0.025% saponin. After further rinsing with PBS, cell monolayers were blocked with PBS containing 4% bovine serum albumin and 10% goat serum. Cell monolayers were incubated overnight at 4° C with 100 μg/mL of mouse monoclonal antibody against ZO-1 (Invitrogen, Camarillo, CA). After at least three washes with PBS, monolayers were incubated for 40 min with 100 μg/mL Alexa fluor 594-labeled goat anti-mouse secondary antibody (Invitrogen). After three rinses, the polycarbonate membrane with cell monolayers was excised from the Transwell® insert using a scalpel and mounted on a glass side with a cover slip. Images were captured using an Olympus Fluoview FV1000 confocal laser scanning microscope.

We used flow cytometry to evaluate the role of surface folic acid in enhancing cellular uptake of nanoparticles. Caco-2 cells (200,000 cells) were suspended in PBS and incubated at 4° C for 30 min with 1 mL of PBS containing 125 μg/mL of 6-coumarin-labeled nanoparticle formulations, in the presence or absence of 20 μM free folic acid. Cell suspensions were then washed thrice with PBS and then incubated further 37° C for 15 min. Flow cytometric analysis was carried out with 488 Laser 530/30 (FL-1). Flow data was analyzed on Cyflogic software.

3. Results

3.1 Characterization of nanoparticles

The particle size of the different nanoparticle formulations ranged from 200 to 300 nm (Table 1). SEM of non-functionalized and folic acid-functionalized nanoparticles revealed their regular and spherical shape (Figure 1). The zeta potential of nanoparticles was negative and ranged from about −10 mV to −13 mV (Table 1). The paclitaxel loading was similar for the three formulations. These results suggested that there were no gross differences in the physical characteristics of the surface functionalized and non-functionalized formulations.

Incorporation of PLA-PEG block co-polymer or the PLA-PEG-folic acid in nanoparticles was confirmed by observing the proton peaks from PEG (CH_2 at 3.5 ppm) in the nanoparticle sample (Figure 2). Free folic acid and PLA-PEG-folic acid showed proton peaks at 11.39 ppm (aromatic hydroxyl group), 8.58 ppm (2-pyrazine CH) and 7.61ppm (1-benzene CH). Because of the extremely low concentration of folic acid in nanoparticles (relative to polymer concentrations), we were unable to detect peaks corresponding to folic acid in nanoparticle samples; however, the presence of PEG peaks in these samples indicate that the PEG-folate conjugate is present in nanoparticles.

3.2 Cellular transport across Caco-2 cell monolayers

In order to investigate the effect of encapsulation in nanoparticles on the transepithelial transport of paclitaxel, permeation of nanoparticle-encapsulated and free paclitaxel across Caco-2 cell monolayers were determined. In order to confirm the suitability of using Caco-2 cells as an *in vitro* model for the proposed studies, we determined P-gp expression in these cells. As can be seen from the Western blotting data (Figure 3A), this cell line was characterized by robust expression of P-gp. Similarly, flow cytometry studies showed that these cells were characterized by high expression of the folic acid receptor (Figure 3B).

Figure 4 shows the P_{app} of paclitaxel after 2 h and 6 h of incubation. After 2 h, the P_{app} of paclitaxel was similar for all the treatments. After incubation for 6 h, however, paclitaxel transport was significantly higher for all the nanoparticle formulations compared to that for the free drug. Encapsulation in nanoparticles, with or without PEG, increased paclitaxel transport five-fold, while encapsulation in folic acid-functionalized nanoparticles increased the transport by eight-fold.

The transepithelial electrical resistance (TEER) was monitored to ensure that cell confluency and integrity were maintained throughout the experiment. As shown in figure 5, the TEER values were not affected significantly (less than 10% of reduction) by any of the nanoparticle formulations. This suggests that increased paclitaxel transport was not because of loss in monolayer integrity or opening of tight junctions.

3.3 Cellular uptake in Caco-2 cell monolayers

To further determine the possibility of transcellular transport of nanoparticles across the monolayer, we studied the intracellular uptake of paclitaxel in the monolayer. After 2 h of incubation, intracellular accumulation of paclitaxel was 1.5-fold higher for folic acid - functionalized nanoparticles (Figure 6; $p<0.05$) than for the free drug. The drug accumulation was much higher with nanoparticle formulations (3.5–4.0-fold) than with free drug treatment after 6 h of incubation.

Confocal microscopy was used to further confirm the cellular internalization of nanoparticles. Nanoparticles loaded with a green fluorescence label, 6-coumarin, were used in the study. Figure 7 shows confocal microscopy images of Caco-2 cell monolayers after incubation with nanoparticles and free 6-coumarin (equivalent concentration). Treatment with free 6-coumarin resulted in negligible green fluorescence, which is in agreement with that observed by others [29, 30]. In the case of nanoparticle treatments, green fluorescence was observed around the nucleus but within the cellular space bounded by tight junctions, suggesting the cellular internalization of nanoparticles. Nanoparticle-associated green fluorescence was observed through the entire cross-section of the monolayers. As expected, tight junction-associated red fluorescence was seen to a greater extent on the apical side (figure 6A) than in the interior cross sections (figure 6B) of the monolayer. Similar intensities of tight junction-associated fluorescence were observed after 2 h incubation with free 6-coumarin and for nanoparticle formulations. This further confirms that nanoparticles did not disrupt the Caco-2 cell monolayer and that paracellular transport was not likely.

In order to ascertain that the difference between folic acid-functionalized nanoparticles and non-functionalized nanoparticles is attributable to folic acid functionalization, we determined the uptake of different nanoparticle formulations in the presence and absence of excess folic acid. Flow cytometry data indicated that folic acid functionalized nanoparticles were taken up by Caco-2 cells to a greater extent than other nanoparticle formulations, and that this enhancement in uptake was eliminated in the presence of excess folic acid (Figure 8). These studies provide additional evidence for the role of folic acid functionalization in increasing the uptake of nanoparticles in Caco-2 cells.

4. Discussion

Paclitaxel has poor oral bioavailability because of its active efflux by P-gp, a membrane-bound efflux transporter present on the apical side of the intestinal epithelial cells. Studies in *mdr 1a* (−/−) knockout mice lacking intestinal P-gp showed that the bioavailability of paclitaxel increased from 11% in wild-type mice to 35% in *mdr1a* (−/−) knockout mice [31]. Similarly, other studies have shown improved bioavailability following co-administration of paclitaxel with specific P-gp inhibitors such as cyclosporine A or with excipients that inhibit P-gp efflux [32–36]. Another factor that may account for the low oral bioavailability of paclitaxel is first-pass elimination by cytochrome P450 isoenzymes CYP2C8 and CYP3A4, which metabolize paclitaxel to 6α-hydroxypaclitaxel and 3ρ-hydroxypaclitaxel, respectively [35–38].

Encapsulation of paclitaxel in polymeric nanoparticles could potentially overcome both P-gp mediated drug efflux and first pass metabolism. Previous studies have shown that

nanoparticles can cross the intestinal barrier through two possible mechanisms: paracellular and/or transcellular transport [13]. A number of studies have shown that in the case of PLGA nanoparticles, the transcellular route, which is primarily mediated through transcytosis, predominates [39–43]. The aim of the current work was to explore the effects of folic acid functionalization on the transport of nanoparticle-encapsulated paclitaxel across Caco-2 monolayer, a well-accepted model of the intestinal epithelial barrier [22, 23].

PLGA was used in the formulation because of its biocompatibility and biodegradability. PLGA nanoparticles can be used to encapsulate both hydrophobic small molecules and hydrophilic macromolecules [39]. Moreover, PLGA nanoparticles have the potential to increase the oral bioavailability of several drugs [4–11]. Folic acid was chosen as the surface ligand because it is stable and has the ability to be transcytosed [44]. Importantly, intestinal epithelial cells express folic acid receptors [45], allowing enhanced delivery of folate functionalized delivery systems to and across these cells [46, 47].

Nanoparticles were functionalized with folic acid by a simple interfacial technique we reported before [19]. Presence of PEG and folic acid in the polymer conjugate and in nanoparticles were confirmed by NMR. Further, we have performed extensive characterization studies (transmission electron microscopy, surface plasmon resonance, cell uptake) previously to show the presence of PEG and folic acid on the surface of nanoparticles fabricated using this technique [18, 19]. Addition of PEG and folic acid on the surface of nanoparticles did not significantly affect important physical properties of particles such as particle size, polydispersity, surface charge or drug loading. These results indicate that enhancement in transport observed for folic acid functionalized nanoparticles could be attributed to the presence of folic acid on the surface and not any other physical characteristics. Stability studies indicated that folic acid was stable in simulated gastric and intestinal fluids for at least 6 h (see Supplementary Information).

Encapsulation of paclitaxel in PLGA nanoparticles significantly improved the transport of paclitaxel across Caco-2 cell monolayers. This increase could be the consequence of transcellular transport of nanoparticles across the monolayer. It is also possible that nanoparticles release the encapsulated drug intracellularly, which then diffuses into the basolateral side. Previous studies have shown that PLGA nanoparticles are taken up by intestinal epithelial cells through endocytosis [48–50]. We also observed significantly higher levels of intracellular (total) paclitaxel following treatment with nanoparticle formulations. However, the short time frame (6 h) of the transport study argues against significant drug release within the cell as we have previously shown that PLGA nanoparticles release <10% of the encapsulated drug in the first 6 hrs [21]. Further, we have shown that paclitaxel released from PLGA nanoparticles intracellularly is susceptible to P-gp mediated drug efflux [21]. Thus, if the drug was released inside the cells, it is likely that it will be effluxed into the apical chamber rather than diffuse into the basolateral side.

Paclitaxel transport across the cells was further enhanced with folic acid functionalized nanoparticles. Flow cytometry studies showing the expression of folate receptors and the reduction in uptake of folic acid functionalized nanoparticles in the presence of excess folic acid suggest that enhanced uptake of these nanoparticles is attributable to the presence of folic acid on nanoparticle surface. Folic acid can enter the cells by two distinct routes. The reduced folate carrier is a facilitated transport protein that transports reduced folate molecules into the cell [51]. This carrier is found in most cells but does not transport folate conjugates. Some cells, including intestinal epithelial cells and many malignant cells, also express the folate receptor that exhibits high affinity for folic acid [52, 53]. Folate receptors associate with folate and folate conjugates at the cell surface and internalize them into the cell by caveolae-mediated endocytosis [39]. While several studies have shown increased

cellular uptake of folate-conjugated delivery systems, there is only limited direct evidence for folate conjugation resulting in enhanced transcytosis [54]. However, folate receptors are associated with caveolae, which have been shown to be directly involved in transcytosis.

Transepithelial electrical resistance (TEER) across the monolayer was measured before and during experiments to determine the quality of cellular tight junctions. Cell monolayers were typically used when TEER values were greater at 250 $\Omega.cm^{-1}$, a value considered to reflect the formation of tight junctions between cells [55]. Typically, a 20% decrease in TEER value indicates the opening of tight junctions and/or a compromise in monolayer integrity. In our experiments, we did not see significant changes in TEER values. This argues that nanoparticle formulations did not open tight junctions and paracellular transport is not a possible mechanism of transport. This result is in accordance with previous studies that demonstrated that PLGA nanoparticles have no effect on tight junctions [41].

5. Conclusion

Folic acid-conjugated PLGA nanoparticles significantly increased the permeability of paclitaxel (a BCS class IV drug) across Caco-2 cell monolayers. Folic acid functionalization may enhance the transcellular transport of nanoparticles, and this in turn could have caused the increased drug transport across the monolayers. Future studies will examine the effect of folic acid functionalization on the oral bioavailability of nanoparticle- encapsulated paclitaxel *in vivo*.

Supplementary Material

Refer to Web version on PubMed Central for supplementary material.

Acknowledgments

Funding from NIH (R01AI080928). We thank James Fisher (Clinical Pharmacology Analytical Services, UMN) for help with LC-MS analysis.

References

1. Barrand MA, Bagrij T, Neo SY. Multidrug resistance-associated protein: a protein distinct from P-glycoprotein involved in cytotoxic drug expulsion. Gen Pharmacol. 1997; 28(5):639–45. [PubMed: 9184795]
2. Scripture CD, Sparreboom A, Figg WD. Modulation of cytochrome P450 activity: implications for cancer therapy. Lancet Oncol. 2005; 6(10):780–9. [PubMed: 16198984]
3. Maincent P, Devissaguet JP, LeVerge R, Sado PA, Couvreur P. Preparation and in vivo studies of a new drug delivery system. Nanoparticles of alkylcyanoacrylate. Appl Biochem Biotechnol. 1984; 10:263–5. [PubMed: 6524931]
4. Anand P, Nair HB, Sung B, Kunnumakkara AB, Yadav VR, Tekmal RR, Aggarwal BB. Design of curcumin-loaded PLGA nanoparticles formulation with enhanced cellular uptake, and increased bioactivity in vitro and superior bioavailability in vivo. Biochem Pharmacol. 2010; 79(3):330–8. [PubMed: 19735646]
5. He W, Horn SW, Hussain MD. Improved bioavailability of orally administered mifepristone from PLGA nanoparticles. Int J Pharm. 2007; 334(1–2):173–8. [PubMed: 17101249]
6. Jiao Y, Ubrich N, Marchand-Arvier M, Vigneron C, Hoffman M, Lecompte T, Maincent P. In vitro and in vivo evaluation of oral heparin-loaded polymeric nanoparticles in rabbits. Circulation. 2002; 105(2):230–5. [PubMed: 11790706]
7. Kalaria DR, Sharma G, Beniwal V, Ravi Kumar MN. Design of biodegradable nanoparticles for oral delivery of doxorubicin: in vivo pharmacokinetics and toxicity studies in rats. Pharm Res. 2009; 26(3):492–501. [PubMed: 18998202]

8. Kumar G, Sharma S, Shafiq N, Pandhi P, Khuller GK, Malhotra S. Pharmacokinetics and tissue distribution studies of orally administered nanoparticles encapsulated ethionamide used as potential drug delivery system in management of multi-drug resistant tuberculosis. Drug Deliv. 2011; 18(1): 65–73. [PubMed: 20735202]
9. Mittal G, Carswell H, Brett R, Currie S, Kumar MN. Development and evaluation of polymer nanoparticles for oral delivery of estradiol to rat brain in a model of Alzheimer's pathology. J Control Release. 2011; 150(2):220–8. [PubMed: 21111014]
10. Mittal G, Sahana DK, Bhardwaj V, Ravi Kumar MN. Estradiol loaded PLGA nanoparticles for oral administration: effect of polymer molecular weight and copolymer composition on release behavior in vitro and in vivo. J Control Release. 2007; 119(1):77–85. [PubMed: 17349712]
11. Zhao L, Feng SS. Enhanced oral bioavailability of paclitaxel formulated in vitamin E-TPGS emulsified nanoparticles of biodegradable polymers: in vitro and in vivo studies. J Pharm Sci. 2010; 99(8):3552–60. [PubMed: 20564384]
12. des Rieux A, Ragnarsson EG, Gullberg E, Preat V, Schneider YJ, Artursson P. Transport of nanoparticles across an in vitro model of the human intestinal follicle associated epithelium. Eur J Pharm Sci. 2005; 25(4–5):455–65. [PubMed: 15946828]
13. Plapied L, Duhem N, des Rieux A, Préat V. Fate of polymeric nanocarriers for oral drug delivery. Curr Opin Colloid Interface Sci. 2011; 16(3):228–37.
14. Roger E, Lagarce F, Garcion E, Benoit JP. Lipid nanocarriers improve paclitaxel transport throughout human intestinal epithelial cells by using vesicle-mediated transcytosis. J Control Release. 2009; 140(2):174–81. [PubMed: 19699246]
15. Roger E, Lagarce F, Garcion E, Benoit JP. Biopharmaceutical parameters to consider in order to alter the fate of nanocarriers after oral delivery. Nanomedicine (Lond). 2010; 5(2):287–306. [PubMed: 20148639]
16. Snoeck V, Goddeeris B, Cox E. The role of enterocytes in the intestinal barrier function and antigen uptake. Microbes Infect. 2005; 7(7–8):997–1004. [PubMed: 15925533]
17. Hillaireau H, Couvreur P. Nanocarriers' entry into the cell: relevance to drug delivery. Cell Mol Life Sci. 2009; 66(17):2873–96. [PubMed: 19499185]
18. Patil Y, Sadhukha T, Ma L, Panyam J. Nanoparticle-mediated simultaneous and targeted delivery of paclitaxel and tariquidar overcomes tumor drug resistance. J Control Release. 2009; 136(1):21–9. [PubMed: 19331851]
19. Patil YB, Toti US, Khdair A, Ma L, Panyam J. Single-step surface functionalization of polymeric nanoparticles for targeted drug delivery. Biomaterials. 2009; 30(5):859–66. [PubMed: 19019427]
20. Salem AK, Cannizzaro SM, Davies MC, Tendler SJ, Roberts CJ, Williams PM, Shakesheff KM. Synthesis and characterisation of a degradable poly(lactic acid)-poly(ethylene glycol) copolymer with biotinylated end groups. Biomacromol. 2001; 2(2):575–80.
21. Chavanpatil MD, Patil Y, Panyam J. Susceptibility of nanoparticle-encapsulated paclitaxel to P-glycoprotein-mediated drug efflux. Int J Pharm. 2006; 320(1–2):150–6. [PubMed: 16713148]
22. Artursson P, Borchardt RT. Intestinal drug absorption and metabolism in cell cultures: Caco-2 and beyond. Pharm Res. 1997; 14(12):1655–8. [PubMed: 9453050]
23. Artursson P, Karlsson J. Correlation between oral drug absorption in humans and apparent drug permeability coefficients in human intestinal epithelial (Caco-2) cells. Biochem Biophys Res Commun. 1991; 175(3):880–5. [PubMed: 1673839]
24. Gao X, Chen J, Tao W, Zhu J, Zhang Q, Chen H, Jiang X. UEA I-bearing nanoparticles for brain delivery following intranasal administration. Int J Pharm. 2007; 340(1–2):207–15. [PubMed: 17499948]
25. Panyam J, Sahoo SK, Prabha S, Bargar T, Labhasetwar V. Fluorescence and electron microscopy probes for cellular and tissue uptake of poly(D,L-lactide-co-glycolide) nanoparticles. Int J Pharm. 2003; 262(1–2):1–11. [PubMed: 12927382]
26. Qaddoumi MG, Ueda H, Yang J, Davda J, Labhasetwar V, Lee VH. The characteristics and mechanisms of uptake of PLGA nanoparticles in rabbit conjunctival epithelial cell layers. Pharm Res. 2004; 21(4):641–8. [PubMed: 15139521]

27. Zhao J, Liu CS, Yuan Y, Tao XY, Shan XQ, Sheng Y, Wu F. Preparation of hemoglobin-loaded nano-sized particles with porous structure as oxygen carriers. Biomaterials. 2007; 28(7):1414–22. [PubMed: 17126898]
28. Davda J, Labhasetwar V. Characterization of nanoparticle uptake by endothelial cells. Int J Pharm. 2002; 233(1–2):51–9. [PubMed: 11897410]
29. Dong Y, Feng SS. Poly(d,l-lactide-co-glycolide)/montmorillonite nanoparticles for oral delivery of anticancer drugs. Biomaterials. 2005; 26(30):6068–76. [PubMed: 15894372]
30. Eley JG, Pujari VD, McLane J. Poly (lactide-co-glycolide) nanoparticles containing coumarin-6 for suppository delivery: in vitro release profile and in vivo tissue distribution. Drug Deliv. 2004; 11(4):255–61. [PubMed: 15371107]
31. Sparreboom A, van Asperen J, Mayer U, Schinkel AH, Smit JW, Meijer DK, Borst P, Nooijen WJ, Beijnen JH, van Tellingen O. Limited oral bioavailability and active epithelial excretion of paclitaxel (Taxol) caused by P-glycoprotein in the intestine. Proc Natl Acad Sci U S A. 1997; 94(5):2031–5. [PubMed: 9050899]
32. Ho PY, Yeh TK, Yao HT, Lin HL, Wu HY, Lo YK, Chang YW, Chiang TH, Wu SH, Chao YS, Chen CT. Enhanced oral bioavailability of paclitaxel by D-alpha-tocopheryl polyethylene glycol 400 succinate in mice. Int J Pharm. 2008; 359(1–2):174–81. [PubMed: 18513900]
33. Mathot F, des Rieux A, Arien A, Schneider YJ, Brewster M, Preat V. Transport mechanisms of mmePEG750P(CL-co-TMC) polymeric micelles across the intestinal barrier. J Control Release. 2007; 124(3):134–43. [PubMed: 17928087]
34. Terwogt JM, Nuijen B, Huinink WW, Beijnen JH. Alternative formulations of paclitaxel. Cancer Treat Rev. 1997; 23(2):87–95. [PubMed: 9225960]
35. Woo JS, Lee CH, Shim CK, Hwang SJ. Enhanced oral bioavailability of paclitaxel by coadministration of the P-glycoprotein inhibitor KR30031. Pharm Res. 2003; 20(1):24–30. [PubMed: 12608532]
36. Zastre JA, Jackson JK, Wong W, Burt HM. P-glycoprotein efflux inhibition by amphiphilic diblock copolymers: relationship between copolymer concentration and substrate hydrophobicity. Mol Pharm. 2008; 5(4):643–53. [PubMed: 18380467]
37. Schellens JH, Malingre MM, Kruijtzer CM, Bardelmeijer HA, van Tellingen O, Schinkel AH, Beijnen JH. Modulation of oral bioavailability of anticancer drugs: from mouse to man. Eur J Pharm Sci. 2000; 12(2):103–10. [PubMed: 11102737]
38. van Asperen J, van Tellingen O, van der Valk MA, Rozenhart M, Beijnen JH. Enhanced oral absorption and decreased elimination of paclitaxel in mice cotreated with cyclosporin A. Clin Cancer Res. 1998; 4(10):2293–7. [PubMed: 9796957]
39. Bala I, Hariharan S, Kumar MN. PLGA nanoparticles in drug delivery: the state of the art. Critical Rev Ther Drug Carrier Sys. 2004; 21(5):387–422.
40. Behrens I, Pena AI, Alonso MJ, Kissel T. Comparative uptake studies of bioadhesive and non-bioadhesive nanoparticles in human intestinal cell lines and rats: the effect of mucus on particle adsorption and transport. Pharm Res. 2002; 19(8):1185–93. [PubMed: 12240945]
41. Cartiera MS, Johnson KM, Rajendran V, Caplan MJ, Saltzman WM. The uptake and intracellular fate of PLGA nanoparticles in epithelial cells. Biomaterials. 2009; 30(14):2790–8. [PubMed: 19232712]
42. Fillafer C, Friedl DS, Wirth M, Gabor F. Fluorescent bionanoprobes to characterize cytoadhesion and cytoinvasion. Small. 2008; 4(5):627–33. [PubMed: 18491364]
43. Weissenboeck A, Bogner E, Wirth M, Gabor F. Binding and uptake of wheat germ agglutinin-grafted PLGA-nanospheres by caco-2 monolayers. Pharm Res. 2004; 21(10):1917–23. [PubMed: 15553240]
44. Bareford LM, Swaan PW. Endocytic mechanisms for targeted drug delivery. Adv Drug Deliv Rev. 2007; 59(8):748–58. [PubMed: 17659804]
45. Vincent ML, Russell RM, Sasak V. Folic acid uptake characteristics of a human colon carcinoma cell line, Caco-2. A newly-described cellular model for small intestinal epithelium. Hum Nutr Clin Nutr. 1985; 39(5):355–60. [PubMed: 4055425]

46. Anderson KE, Eliot LA, Stevenson BR, Rogers JA. Formulation and evaluation of a folic acid receptor-targeted oral vancomycin liposomal dosage form. Pharm Res. 2001; 18(3):316–22. [PubMed: 11442271]
47. Anderson KE, Stevenson BR, Rogers JA. Folic acid-PEO-labeled liposomes to improve gastrointestinal absorption of encapsulated agents. J Control Release. 1999; 60(2–3):189–98. [PubMed: 10425325]
48. Gaumet M, Gurny R, Delie F. Localization and quantification of biodegradable particles in an intestinal cell model: the influence of particle size. Eur J Pharm Sci. 2009; 36(4–5):465–73. [PubMed: 19124077]
49. Jani P, Halbert GW, Langridge J, Florence AT. Nanoparticle uptake by the rat gastrointestinal mucosa: quantitation and particle size dependency. J Pharm Pharmacol. 1990; 42(12):821–6. [PubMed: 1983142]
50. Jepson MA, Simmons NL, O'Hagan DT, Hirst BH. Comparison of poly(DL-lactide-co-glycolide) and polystyrene microsphere targeting to intestinal M cells. J Drug Target. 1993; 1(3):245–9. [PubMed: 8069566]
51. Xia W, Low PS. Folate-targeted therapies for cancer. J Med Chem. 2010; 53(19):6811–24. [PubMed: 20666486]
52. Kumari A, Yadav SK. Cellular interactions of therapeutically delivered nanoparticles. Expert Opin Drug Deliv. 2011; 8(2):141–51. [PubMed: 21219249]
53. Wang S, Low PS. Folate-mediated targeting of antineoplastic drugs, imaging agents, and nucleic acids to cancer cells. J Control Release. 1998; 53(1–3):39–48. [PubMed: 9741912]
54. Sandoval RM, Kennedy MD, Low PS, Molitoris BA. Uptake and trafficking of fluorescent conjugates of folic acid in intact kidney determined using intravital two-photon microscopy. Am J Physiol Cell Physiol. 2004; 287(2):C517–26. [PubMed: 15102609]
55. Artursson P. Epithelial transport of drugs in cell culture. I: A model for studying the passive diffusion of drugs over intestinal absorptive (Caco-2) cells. J Pharm Sci. 1990; 79(6):476–82. [PubMed: 1975619]

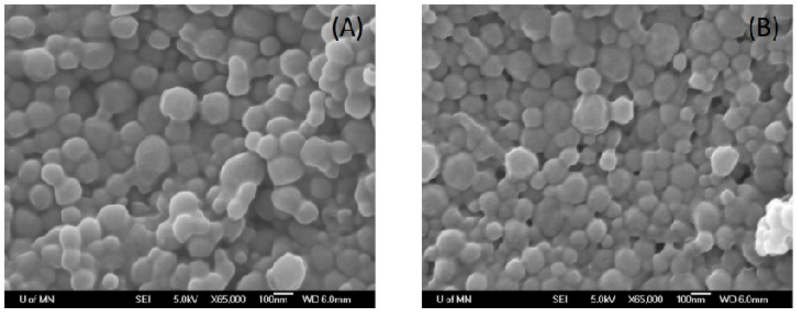

Figure 1.
Representative scanning electron micrograph of non–functionalized nanoparticles (**A**) and folic acid-functionalized nanoparticles (**B**).

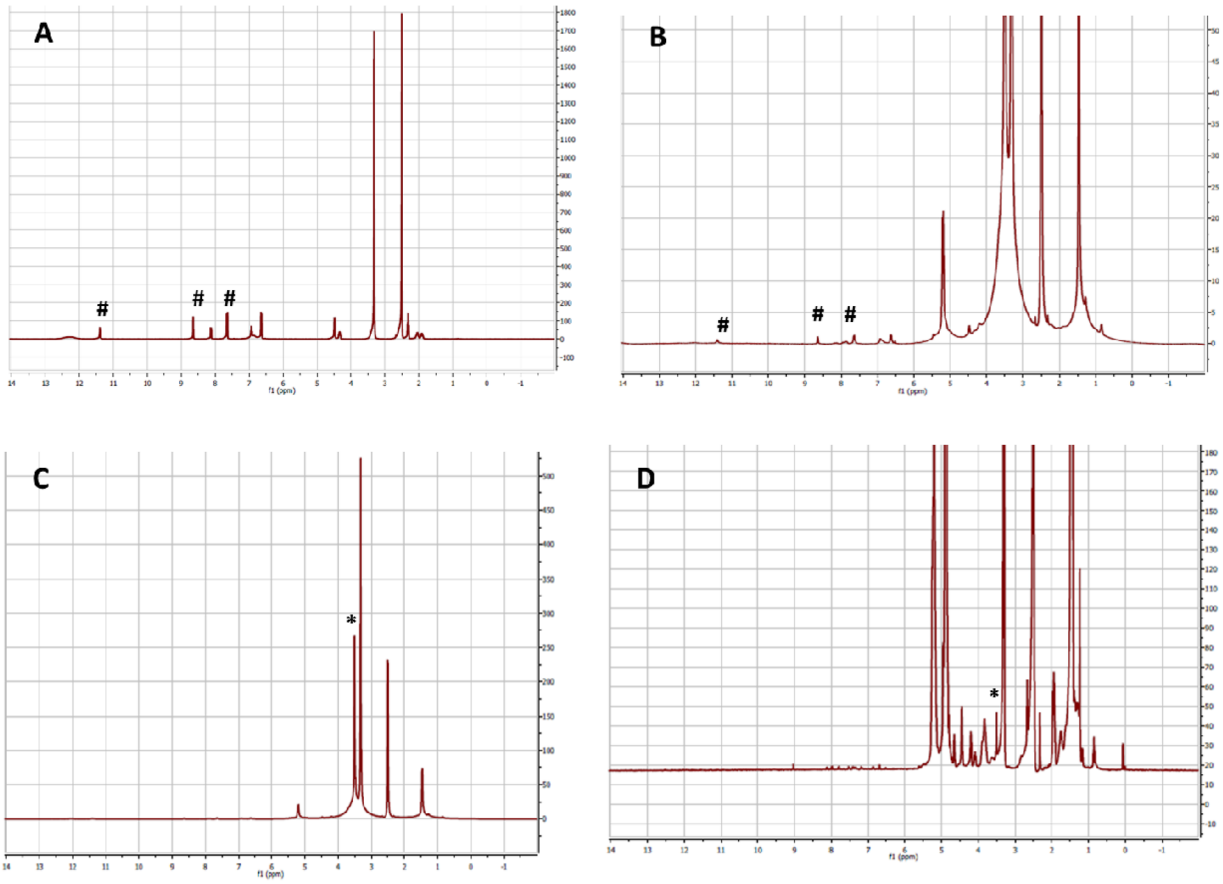

Figure 2.
Proton NMR of (a) free folic acid; (b) and (c) PLA-PEG-folic acid; and (d) PLA-PEG-folic acid functionalized NP. The NMR spectrum in (c) is expanded in (b) to show the peaks corresponding to folic acid. # indicate folic acid peaks; * indicate PEG peaks.

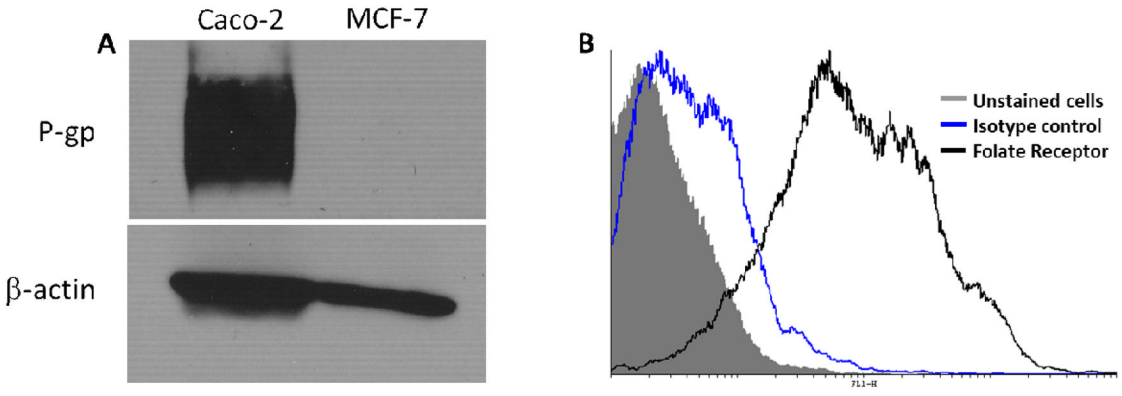

Figure 3.

Characterization of Caco-2 cells for (A) P-gp expression and (B) folate receptor expression. (A) Western blotting was used to characterize P-gp expression in Caco-2 and MCF-7 (negative control) cells. β-actin served as the loading control. (B) Flow cytometry was used to characterize the folate receptor expression in Caco-2 cells. Cells were stained with either mouse anti-folate receptor antibody or mouse IgG2b k isotype control, followed by FITC-labeled goat–anti-mouse secondary antibody. Flow cytometric analysis was carried out with 488 Laser 530/30(FL-1) to enable FITC discrimination.

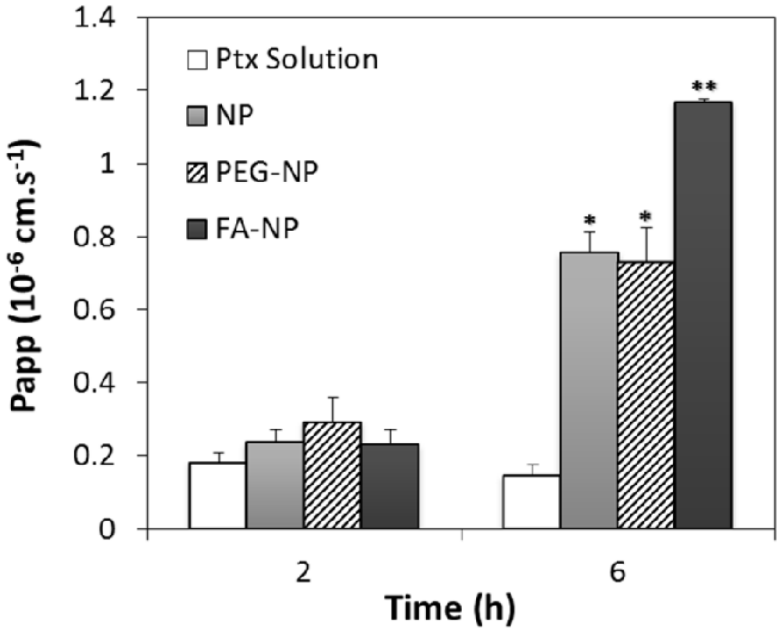

Figure 4.

Apparent permeability coefficients (P_{app}) of different paclitaxel (Ptx) formulations: Ptx solution, Ptx-loaded non-functionalized nanoparticles (NP), Ptx-loaded, PEG functionalized nanoparticles (PEG-NP), Ptx-loaded, folic acid-PEG-functionalized nanoparticles (FA-NP). Transport study was conducted using Caco-2 monolayers as described in the Methods section (n=4; data shown is mean ± SD, * $p<0.05$ in comparison with Ptx solution, ** $p<0.05$ in comparison with NP and PEG-NP).

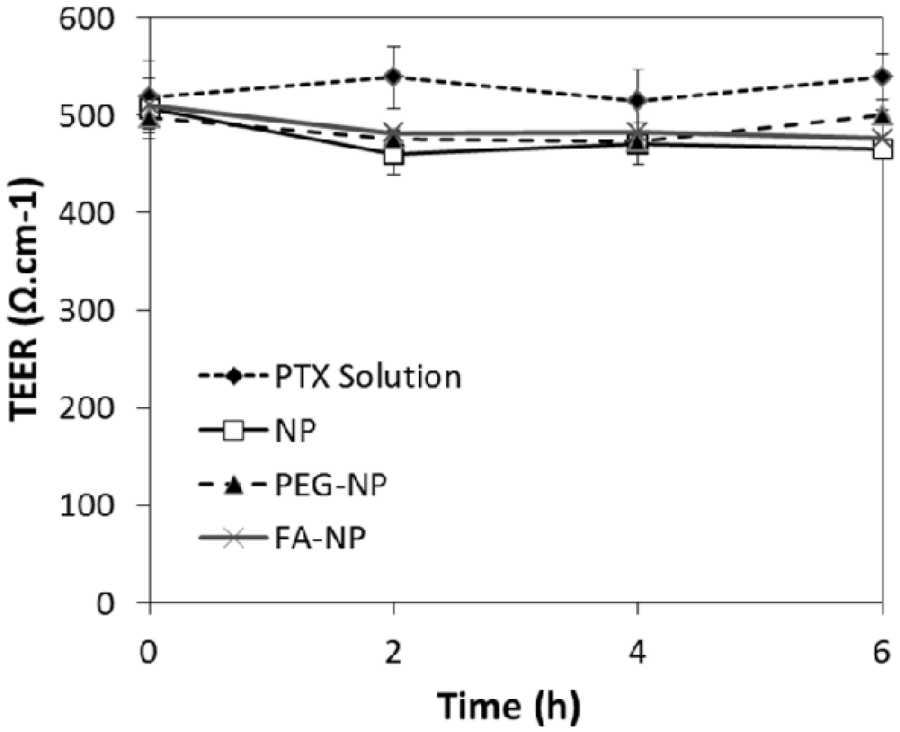

Figure 5.
Effect of different treatments on the TEER across the Caco-2 monolayers. Legend: paclitaxel solution - Ptx solution; Ptx-loaded non-functionalized nanoparticles - NP, Ptx-loaded, PEG-functionalized nanoparticles - PEG-NP, Ptx-loaded, folic acid-PEG-functionalized nanoparticles - FA-NP.

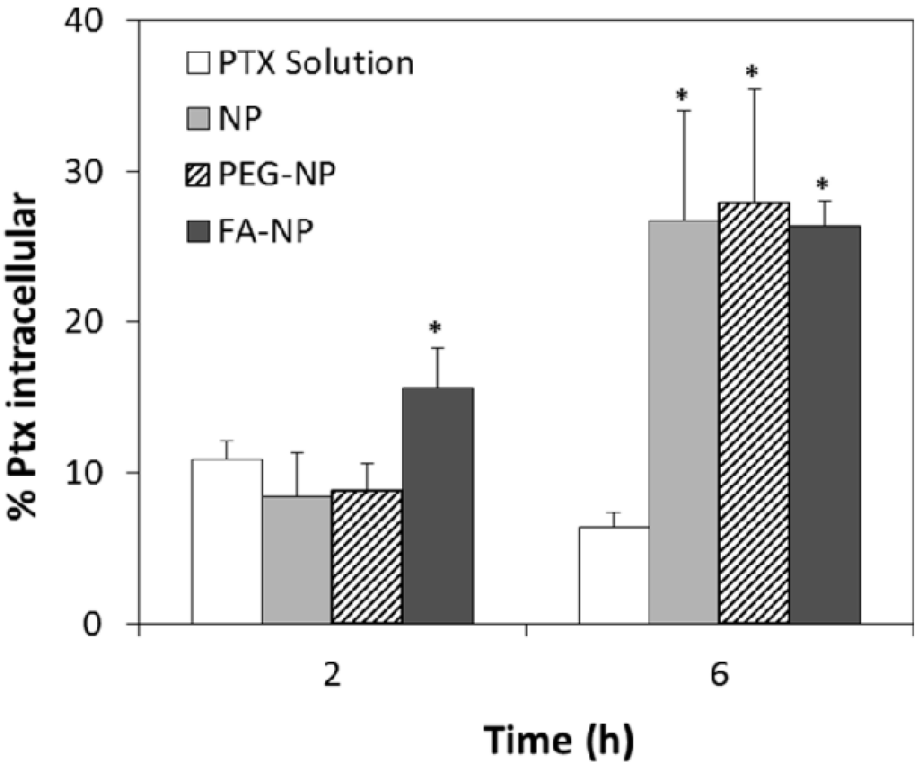

Figure 6.
Effect of encapsulation in nanoparticles on paclitaxel uptake by Caco-2 cells (n=4; data showed is mean ± SD, * $p<0.05$ in comparison with Ptx solution). Legend: paclitaxel solution - Ptx solution; Ptx-loaded non-functionalized nanoparticles - NP, Ptx-loaded, PEG functionalized nanoparticles - PEG-NP, Ptx-loaded, folic acid-PEG-functionalized nanoparticles - FA-NP.

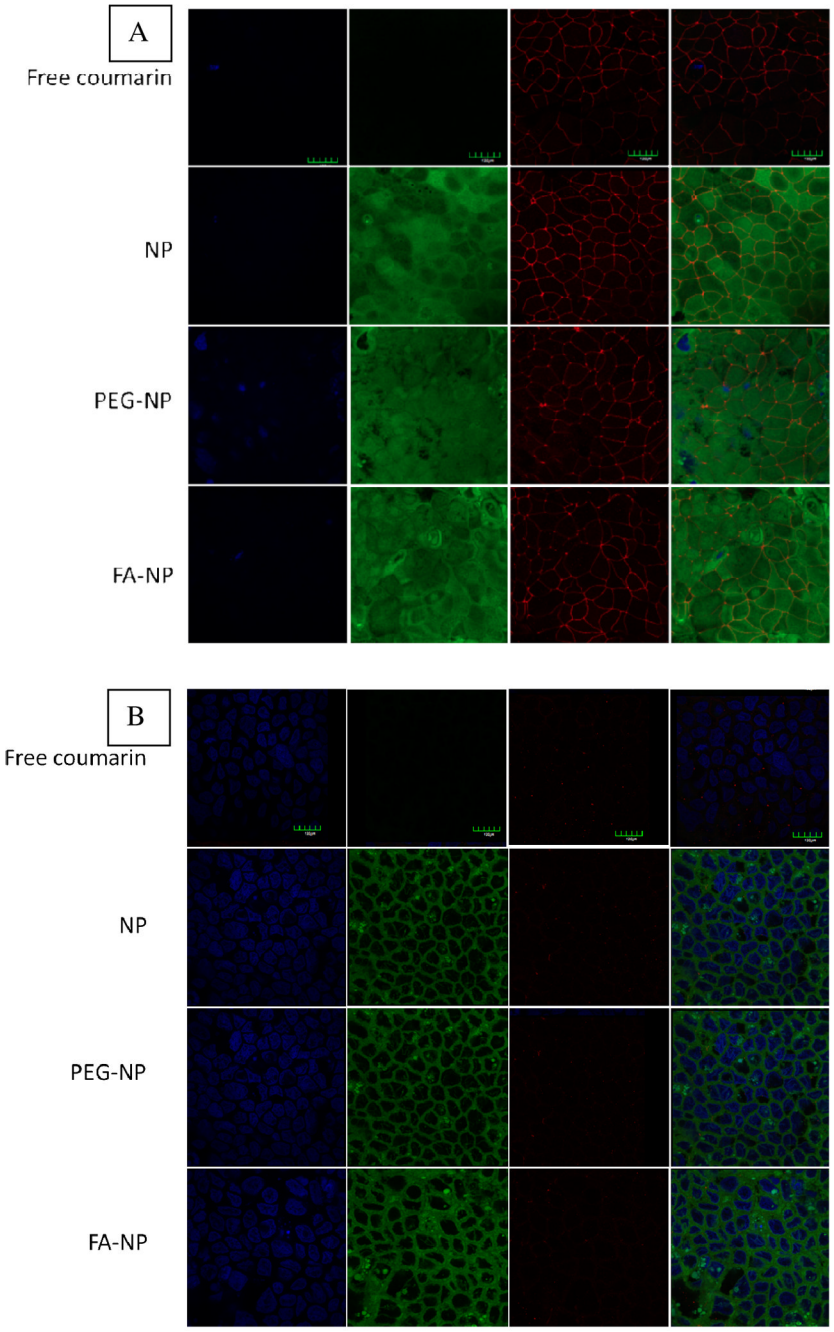

Figure 7.
Nanoparticle uptake in Caco-2 cells after 6 h of incubation. (A) Apical side and (B) intracellular images. Blue channel represents nuclei stained with DAPI (column 1), green channel indicates 6-coumarin fluorescence (column 2), red channel denotes the cell perimeter highlighted by tight junctions labeled with antibody against ZO-1 coupled with Alexa fluor 594 (column 3). Overlay of the three channels are shown in column 4. Scale bar represents 150 μm.

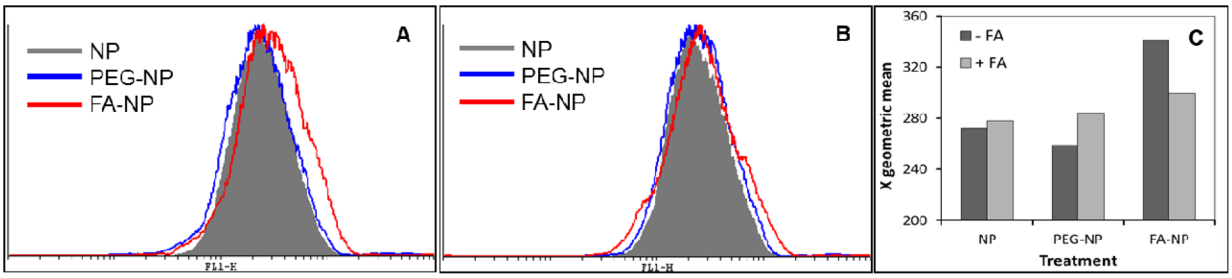

Figure 8.

Flow cytometric analysis showing that (A) folic acid functionalization increases the cellular internalization of nanoparticles and (B) presence of excess folic acid (20 μM) eliminates the enhancement in uptake provided by folic acid functionalization. (C) Effect of excess folic acid on the geometric mean of the fluorescence intensities in cells treated with different nanoparticle formulations. Caco-2 cells (250,000) were incubated with nanoparticle formulations (125 μg/mL) at 4° C for 30 min, followed by at 37° C for 15 min, and then analyzed on a flow cytometer.

Table 1

Characterization of nanoparticles

Formulation [a]	Size (nm)	PDI [b]	Zeta potential [c] (mV)	Paclitaxel loading (μg/mg)
NP	268	0.233	−13.46	13.2 ± 2.9
PEG-NP	296	0.269	−10.41	12.0 ± 1.3
FA-NP	213	0.276	−13.31	13.0 ± 2.0

[a] NP - Non-functionalized nanoparticles; PEG-NP - PEG functionalized nanoparticles; FA-NP - folic acid-PEG-functionalized nanoparticles;

[b] PDI – polydispersity index;

[c] measured in deionized water